

Time Series (re)sampling using Generative Adversarial Networks*

Christian M. Dahl[†] Emil N. Sørensen[‡]

February 2, 2021

Abstract

We propose a novel bootstrap procedure for dependent data based on Generative Adversarial networks (GANs). We show that the dynamics of common stationary time series processes can be learned by GANs and demonstrate that GANs trained on a single sample path can be used to generate additional samples from the process. We find that temporal convolutional neural networks provide a suitable design for the generator and discriminator, and that convincing samples can be generated on the basis of a vector of iid normal noise. We demonstrate the finite sample properties of GAN sampling and the suggested bootstrap using simulations where we compare the performance to circular block bootstrapping in the case of resampling an AR(1) time series processes. We find that resampling using the GAN can outperform circular block bootstrapping in terms of empirical coverage.

*Acknowledgements: The authors gratefully acknowledge support from the Google Tensorflow Research Cloud (TFRC). PyTorch code for this paper is available on request. We also thank Giovanni Mellace and Peter Sandholt Jensen for useful comments.

[†]Department of Business and Economics, University of Southern Denmark, cmd@sam.sdu.dk

[‡]School of Economics, University of Bristol, e.sorensen@bristol.ac.uk

1. INTRODUCTION

Generative Adversarial Nets (GANs) were introduced by Goodfellow, Pouget-Abadie, et al. (2014). Based on an initial training sample, GANs can learn to generate additional data that looks similar. GANs are intensely researched in the deep learning literature (Radford et al., 2015; Salimans et al., 2016; Gulrajani et al., 2017; Arjovsky et al., 2017) but have received minor attention in time series analysis. There are examples of GANs being explored for structural models (Kaji et al., 2018) and estimation of treatment effects (Athey et al., 2019). However, these are both in the cross-sectional iid setting. Hyland et al. (2017) suggest that GANs can be used for what they call “medical” time series but they lack a clear definition of the data generating process (DGP) and correspondingly measures of quality for the learned model. Recently, Wiese et al. (2020) described a GAN for financial time series that can reproduce some of the stylised facts of such series using a temporal convolution architecture related to the one suggested in this work. Smith and Smith (2020) also outlined a method for training GANs on time series using spectrograms. Unlike Wiese et al. (2020) and Smith and Smith (2020) our focus is on the general applicability of GANs as a bootstrap method for dependent processes. The potential usefulness of GANs for such time series bootstraps is briefly mentioned in recent work by Haas and Richter (2020).

GANs have frequently been applied for image synthesis (Goodfellow, Pouget-Abadie, et al., 2014; Radford et al., 2015; Arjovsky et al., 2017) and the generated samples are often evaluated using measures such as Inception Score (Salimans et al., 2016) or Fréchet Inception Distance (Heusel et al., 2017). Both measures utilise a neural network trained for image recognition to attempt to assess the visual quality of the generated samples. However, these are heuristics and it is difficult to construct a theoretically motivated notion of quality. Contrary to Hyland et al. (2017), we argue that it is straightforward to assess the basic properties of the generated samples in a time series context as the theoretical properties of many time series are well understood – contingent on considering explicitly defined data generating processes. A similar point is made by Wiese et al. (2020).

We show that stationary autoregressive time series processes – exemplified by the AR(1) process – can be learned by GANs trained on a single sample path and find that temporal convolutional neural networks provide a suitable design for the generator and discriminator.

Bootstrapping dependent data – such as samples from a time series process – has received long-standing attention in the literature, see e.g. the overview of block bootstrapping by Lahiri (1999) and the newer contributions of Paparoditis and Politis (2001) and Shao (2010). We suggest that GANs provide a novel approach to such bootstrapping which we call the generative bootstrap (GB). The theoretical properties of GANs – and hence our suggested generative bootstrap – is an active area of research, see (Biau, Cadre, et al., 2018; Biau, Sangnier, et al., 2020; Haas and Richter, 2020) and we instead contribute by analysing the finite sample properties of generative bootstrapping using simulations where we compare the performance against Circular Block Bootstrapping (CBB) (Politis and Romano, 1992) for the AR(1) process. In particular, we recover the parameters of the true data generating process using the simulated data and thereby show that the generative model has learned at least a minimum of characteristics of the process. Further, we find that resampling using the generative model can outperform CBB for dependent data on the empirical coverage of percentile confidence intervals.

Our main contributions are: (1) we show that GANs can learn the dynamics of stationary autoregressive time series processes, (2) we find that temporal convolutions provide a working architecture for the discriminator and generator networks, and (3) we show that GANs can be used to resample from dependent data with suggestive finite-sample improvements in empirical coverage over CBB. (1) and (2) are also discussed by Wiese et al. (2020). However, Wiese et al. (2020) do not consider the more general applicability of GANs to time series bootstrapping which we define and subsequently evaluate in our simulations.

In Section 2 we review two common GANs and discuss how they can be trained to generate samples from a time series based on an initial sample path. Section 3 discusses an algorithm for using the trained GAN to bootstrap dependent data. In Section 4 we provide

simulation evidence of the quality of the learned GAN and the performance when it is used for bootstrapping. Section 5 concludes.

2. GENERATIVE ADVERSARIAL NETS

2.1. Basic GAN

The concept of GANs can be introduced intuitively as follows. Assume that a real sample of data is drawn from the unknown distribution F_X and assume that we have another arbitrary, but known, distribution F_Z . The generator G is a function that transforms a sample from F_Z into a sample that looks like it is drawn from the real data distribution F_X . The discriminator D is a function that tries to determine if a given sample is drawn from the real data distribution F_X or not. The two models are set to play a game against each other. The generator tries to fool the discriminator by generating fake samples that look as real as possible, and the discriminator tries to detect the generator's forgery by determining if it got a real or fake sample.

Let G and D be specified up to the finite dimensional parameters θ_G and θ_D respectively. Also, let x_{real} denote some generic real sample from distribution F_X and $x_{fake} = G(z; \theta_G)$, $z \sim F_Z$ a generated sample.

Goodfellow, Pouget-Abadie, et al. (2014) suggest solving the minimax problem

$$\min_{\theta_G} \max_{\theta_D} \mathbb{E}_{F_X} \log D(x; \theta_D) + \mathbb{E}_{F_Z} \log(1 - D(G(z; \theta_G); \theta_D)). \quad (1)$$

In practice Goodfellow, Pouget-Abadie, et al. (2014) separate the minimisation and maximisation steps into

$$\begin{aligned} & \max_{\theta_D} \mathbb{E}_{F_X} \log D(x; \theta_D) + \mathbb{E}_{F_Z} \log(1 - D(G(z; \theta_G); \theta_D)) \\ & \min_{\theta_G} \mathbb{E}_{F_Z} \log(1 - D(G(z; \theta_G); \theta_D)) \end{aligned}$$

and iterate between these to learn the discriminator and generator using batching and stochastic gradient descent. We skip the details here, but describe the training in detail for the Wasserstein GAN in the following section. Algorithm 1 provides an overview of the training algorithm.

Biau, Cadre, et al. (2018) and Goodfellow, Pouget-Abadie, et al. (2014) argue that, under a set of assumptions, the optimal discriminator in the minimax formulation in Equation 1 is related to the Jensen-Shannon divergence between the distributions of the real and generated data. If F_G is the distribution of the transformation $G(Z; \theta_G)$, $Z \sim F_Z$ and the optimal discriminator is in the class of functions $\{D(\cdot, \theta_D) : \theta_D \in \Theta\}$ where Θ is some parameter space then the solution to the *maximisation* problem in Equation 1 is the Jensen-Shannon divergence JS between F_X and F_G (Biau, Cadre, et al., 2018; Goodfellow, Pouget-Abadie, et al., 2014),

$$\max_{\theta_D \in \Theta} \mathbb{E}_{F_X} \log D(x; \theta_D) + \mathbb{E}_{F_Z} \log(1 - D(G(z; \theta_G); \theta_D)) = 2JS(F_X, F_G) - \log 4 \quad (2)$$

and, heuristically, if we assume the discriminator is optimal then the generator is solving the problem

$$\min_{\theta_G} JS(F_X, F_G). \quad (3)$$

As noted by Biau, Cadre, et al. (2018), this seems to have motivated work on investigating other divergences/distances in the context of GANs. One such distance is the Wasserstein distance which we will consider in the following section.

2.2. Wasserstein GAN

Arjovsky et al. (2017) argue that an alternative distance measure in Equation 3 is the order-1 Wasserstein (Earth-Mover) distance which results in the Wasserstein GAN. Consider informally two probability measures \mathbb{P} and \mathbb{Q} defined on a suitable common probability space

Algorithm 1 GAN (Goodfellow, Pouget-Abadie, et al., 2014)

for $i = 1, 2, \dots, N$ **do**:
 $z \leftarrow \text{Sample}(F_Z)$ ▷ **Discriminator update**
 $x_{fake} \leftarrow G(z; \theta_G)$
 $x_{real} \leftarrow \text{Sample}(\mathcal{X})$ ▷ \mathcal{X} is a given collection of samples from F_X
 $L_D^{(b)} \leftarrow \frac{1}{n_b} \sum_i \log D(x_{real}; \theta_D) + \log(1 - D(x_{fake}; \theta_D))$ ▷ Discriminator loss
 $\theta_D \leftarrow \theta_D - lr_D \nabla_{\theta_D} L_D^{(b)}$ ▷ Parameter update

 $z \leftarrow \text{Sample}(F_Z)$ ▷ **Generator update**
 $x_{fake} \leftarrow G(z; \theta_G)$
 $L_G^{(b)} \leftarrow \frac{1}{n_b} \sum_i \log(1 - D(x_{fake}; \theta_D))$ ▷ Generator loss
 $\theta_G \leftarrow \theta_G - lr_G \nabla_{\theta_G} L_G^{(b)}$ ▷ Parameter update
end for

(\mathcal{M}, \cdot) . The Wasserstein distance W_1 between \mathbb{P} and \mathbb{Q} is defined as

$$W_1(\mathbb{P}, \mathbb{Q}) = \inf_{\mathbb{V} \in \Pi} \mathbb{E}_{\mathbb{V}} \|x - y\| \quad (4)$$

where, with abuse of notation, Π is the set of all joint probability measures $\mathbb{V}(x, y)$ with marginal probabilities $\mathbb{P}(x)$ and $\mathbb{Q}(y)$, and $\|\cdot\|$ is the absolute value norm (Arjovsky et al., 2017). Here $\mathbb{E}_{\mathbb{V}}$ denotes expectation under the probability measure \mathbb{V} . Arjovsky et al. (2017) argue that Equation 4 is equivalent to

$$W_1(\mathbb{P}, \mathbb{Q}) = \sup_{D \in \mathcal{F}} \mathbb{E}_{\mathbb{P}} D(x) - \mathbb{E}_{\mathbb{Q}} D(x) \quad (5)$$

where \mathcal{F} is the set of real-valued Lipschitz functions on \mathcal{M} with Lipschitz constant 1. In Equation 5 we have conveniently denoted the function to be optimised over by D as we can consider it to play the role of a discriminator. Given the discriminator, the generator would like to minimise the distance between the generated data and real data, if the laws of generated and real data are given by \mathbb{P} and \mathbb{Q} then the generator is solving the problem $\inf_G W_1(\mathbb{P}, \mathbb{Q})$. This is analogous to Equation 3 but the Jensen-Shannon divergence JS has been replaced by the Wasserstein distance W_1 . A primary issue in operationalising

Equation 5 is enforcing the Lipschitz condition on D . For example, say we learn D using a neural network, how do we constrain this network to only learn Lipschitz-1 functions? Let G and D be specified up to the finite dimensional parameters θ_G and θ_D respectively. Also, let x_{real} denote some generic real sample from distribution F_X and $x_{fake} = G(z; \theta_G)$, $z \sim F_Z$ a generated sample. Now based on Equation 5 Arjovsky et al. (2017) suggest solving the minimax problem

$$\min_{\theta_G} \max_{\theta_D} \mathbb{E}_{F_X} D(x; \theta_D) - \mathbb{E}_{F_Z} D(G(z; \theta_G); \theta_D) \quad (6)$$

subject to $D(\cdot; \theta_D) \in \mathcal{F}$. A simple training algorithm for solving the problem (6) would be splitting it into a min and max step, and iterate between them (Goodfellow, Pouget-Abadie, et al., 2014)

$$\max_{\theta_D} \mathbb{E}_{F_X} D(x; \theta_D) - \mathbb{E}_{F_Z} D(G(z; \theta_G); \theta_D) \quad (7)$$

$$\min_{\theta_G} -\mathbb{E}_{F_Z} D(G(z; \theta_G); \theta_D). \quad (8)$$

Gulrajani et al. (2017) recognise that a function is Lipschitz-1 if and only if the norm of the gradient is 1 or less everywhere, so they suggest a gradient penalty to enforce the Lipschitz condition in the discriminator

$$P(\theta_D) = \mathbb{E}_{F_{\tilde{x}}} (\|\nabla_{\tilde{x}} D(\tilde{x}; \theta_D)\|_2 - 1)^2$$

where $\|\cdot\|_2$ is the l_2 norm. Note that $\tilde{x} = ax_{real} + (1-a)x_{fake}$ is a convex combination of x_{real} and x_{fake} with uniform random weight $a \sim U(0, 1)$, and we let $F_{\tilde{x}}$ denote the distribution of these convex combinations. This procedure is motivated heuristically in Gulrajani et al. (2017) and is a less computationally intensive way of enforcing the Lipschitz constraint across

all possible x . Under the gradient penalty the discriminator objective function is now

$$\max_{\theta_D} \mathbb{E}_{F_X} D(x; \theta_D) - \mathbb{E}_{F_Z} D(G(z; \theta_G); \theta_D) + \lambda P(\theta_D) \quad (9)$$

where the weight of the gradient penalty is adjusted by the hyper parameter λ .

Let $\{(z_i, x_{i,real})\}_{i=1}^{n_b}$ constitute a (mini) batch of data where z_i is noise sampled from F_Z and $x_{i,real}$ is a real sample. During training we minimise the batch discriminator loss

$$L_D^{(b)} = \frac{1}{n_b} \sum_{i=1}^{n_b} D(x_{i,fake}; \theta_D) - D(x_{i,real}; \theta_D) + \lambda \frac{1}{n_b} \sum_{i=1}^{n_b} (\|\nabla_{\tilde{x}} D(\tilde{x}_i; \theta_D)\|_2 - 1)^2, \quad (D1)$$

$$\tilde{x}_i = ax_{i,real} + (1-a)x_{i,fake}$$

which is the empirical and batched equivalent of Equation 9, and recall that $x_{i,fake} = G(z_i; \theta_G)$. As per usual, the batch gradients $\nabla_{\theta_D} L_D^{(b)}$ serve as unbiased estimates of $\nabla_{\theta_D} L_D$ (i.e. here L_D is the loss over the entire training sample while $L_D^{(b)}$ is the loss in the batch only, so for L_D the sums run over $(1, \dots, n)$ instead of $(1, \dots, n_b)$) which allow us to do stochastic gradient descent on the parameters (θ_D, θ_G) . The first sum in (D1) amounts to the discriminator objective in Arjovsky et al. (2017) while the second sum corresponds to the gradient penalty suggested by Gulrajani et al. (2017).

Similarly, for the generator we minimise the batch generator loss

$$L_G^{(b)} = \frac{1}{n_b} \sum_{i=1}^{n_b} -D(G(z; \theta_G); \theta_D) \quad (G1)$$

corresponding to Equation 8. By alternating between the objectives (D1) and (G1) we can learn the parameters of G and D . The complete training algorithm of Gulrajani et al. (2017) is given in Algorithm 2 in pseudo-code. Notice that during the discriminator updates the gradient is with respect to θ_D and in the generator updates with respect to θ_G . Algorithm 2 uses Stochastic Gradient Descent (SGD) to update the parameters, but more sophisticated optimisation methods could also be applied, e.g. ADAM (Kingma and Ba, 2014).

Algorithm 2 Wasserstein GAN with Gradient Penalty (Arjovsky et al., 2017; Gulrajani et al., 2017).

```

1: for  $i = 1, 2, \dots, N$  do:
2:   for  $j = 1, 2, \dots, N_{discriminator}$  do: ▷ Discriminator updates.
3:      $z \leftarrow \text{Sample}(F_Z)$ 
4:      $x_{fake} \leftarrow G(z; \theta_G)$ 
5:      $x_{real} \leftarrow \text{Sample}(\mathcal{X})$  ▷  $\mathcal{X}$  is a fixed collection of samples from  $F_X$ 
6:
7:      $\tilde{x} \leftarrow ax_{real} + (1 - a)x_{fake}$  ▷  $a$  is drawn from the uniform distribution  $U(0, 1)$ .
8:      $P^{(b)} \leftarrow \frac{1}{n_b} \sum_{b=1}^{n_b} (\|\nabla_{\tilde{x}} D(\tilde{x}; \theta_D)\|_2 - 1)^2$  ▷ Gradient penalty.
9:      $L_D^{(b)} \leftarrow \frac{1}{n_b} \sum_{b=1}^{n_b} D(x_{fake}; \theta_D) - D(x_{real}; \theta_D) + \lambda P^{(b)}$  ▷ Discriminator loss.
10:     $\theta_D \leftarrow \theta_D - lr_D \nabla_{\theta_D} L_D^{(b)}$  ▷ Parameter update,  $lr_D$  is the learning rate.
11:  end for
12:
13:  for  $j = 1, 2, \dots, N_{generator}$  do: ▷ Generator updates.
14:     $z \leftarrow \text{Sample}(F_Z)$ 
15:     $x_{fake} \leftarrow G(z; \theta_G)$ 
16:
17:     $L_G^{(b)} \leftarrow \frac{1}{n_b} \sum_{b=1}^{n_b} -D(x_{fake}; \theta_D)$  ▷ Generator loss.
18:     $\theta_G \leftarrow \theta_G - lr_G \nabla_{\theta_G} L_G^{(b)}$  ▷ Parameter update,  $lr_G$  is the learning rate.
19:  end for
20: end for

```

The GAN formulation above does not necessarily impose how we should parameterise the discriminator D and generator G . However, in practice, they are commonly learned using neural networks with exact parameterisations depending on the application.¹ Hornik et al. (1990) showed that neural networks with fully-connected layers enjoy universal approximation properties and hence are a natural choice. We do not give an introduction to neural networks and their terminology but refer to the textbook treatment by Goodfellow, Bengio, et al. (2016).

Consider a time series process $Y = \{Y_t : t \in \mathcal{T}\}$ indexed by time t . A time series has the defining property that information flow is unidirectional, so the state of the process at time t , Y_t , can only depend on past information (Y_{t-1}, Y_{t-2}, \dots) while the future is unknown. This constraint is useful when we choose the parameterisation of G and D .

The GAN in Hyland et al. (2017) relied on recurrent neural networks (RNNs) to model time series. We pursue a different approach and base the generator and discriminator on stacked dilated temporal convolutions (DTC) used by Oord et al. (2016) for audio generation. We will refer to this as the TC-architecture. The temporal convolutions are similar to conventional convolutions – see (Goodfellow, Bengio, et al., 2016, Chp. 3) – but they enforce the unidirectional flow of information. They were applied to time series forecasting by Borovykh et al. (2017) and Sen et al. (2019). In particular, Borovykh et al. (2017) showed that DTC networks outperform RNNs in several forecasting problems and are easier to train even for long-range dependence. Very recently, Wiese et al. (2020) similarly suggested temporal convolutions based on (Oord et al., 2016) for financial time series modelling with GANs. The dilation of the temporal convolutions increases the receptive field – in context of time series this is the number of lags that the model can accommodate at once – while limiting the number of parameters (Oord et al., 2016; Borovykh et al., 2017).

In practice, temporal convolutions can be implemented as conventional one-dimensional convolutions with appropriate zero-padding applied to the input, see (Oord et al., 2016). If

¹For example, Radford et al. (2015) use convolutions for images while (Athey et al., 2019) use fully-connected layers in the context of treatment effects.

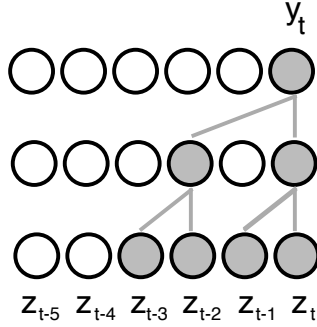


Figure 1: Adapted from Figure 2 in (Oord et al., 2016). An illustration of the DTC network. The output y_t at time t is a function of the present and past noise terms $(z_t, z_{t-1}, z_{t-2}, z_{t-3})$. We generate the output samples as we slide across the noise terms.

we stack d DTC layers with kernel size 2 where the dilation for layer i is 2^i then the total receptive field size at the final layer will be (Yu and Koltun, 2015)

$$p = \sum_{i=1}^d 2^i = 2^{d+1} - 1. \quad (10)$$

For illustration, assume that our generator G consists of d DTC layers. To generate a time series of length b we slide the DTC layers over a sequence of $(b + p)$ iid noise terms

$$(z_1, z_2, \dots, z_{p+b}), \quad z_t \sim F_Z$$

where F_Z is some arbitrarily chosen distribution and p is the receptive field size given in Equation 10. During the GAN training, the parameters in the DTC layers learn to transform this sequence of iid noise into observations from the time series. This is illustrated in Figure 1 for a generator with two DTC layers. On the other hand, the discriminator D considers sequences of observations from the generated or real time series (y_1, y_2, \dots, y_T) and learns the parameters in the DTC layers to distinguish between real and generated samples. We will detail this process in the context of bootstrapping in Section 3, and provide a complete example of the architecture in Section 4.

3. GENERATIVE BOOTSTRAP

We propose the GAN with temporal convolution layers as a method to resample from a time series process. This procedure is called the Generative Bootstrap (GB). The GB is composed of two stages: (1) the GAN is trained on an initial sample from the true DGP using blocking – the *training stage*. (2) samples are generated from the generator of the trained GAN – the *sampling stage*.

The initial sample from the true DGP is re-sampled using a moving block scheme similar to the Moving Block Bootstrap (MBB) (Kunsch, 1989; Liu, Singh, et al., 1992) and n_b of such blocks constitute a batch of data that are used to perform one iteration over the batch losses in Equation D1-G1. Many iterations are performed until the GAN losses stabilise. For sampling, the discriminator is discarded and we feed noise into the generator from an arbitrary distribution F_Z . The generator output is used as a sample to calculate one set of bootstrap statistics. This procedure is repeated for an arbitrary number of samples and the collection of statistics is used to form the GB estimates.

We will see that this differs from conventional block bootstrapping in two respects. Firstly, a conventional MBB would sample blocks of size b with replacement from the initial sample and stack these into one sample path matching the length of the initial sample. This stacked sample is then used to calculate bootstrap statistics. In the GB these blocks are not stacked, but fed as individual samples to train the GAN. Secondly, sampling the GAN does not have to use stacking and the GAN can provide a sample of any size once it has been trained. The size of the sample is determined by the noise terms supplied to the generator.

We proceed to discuss the training and sampling stages below. Algorithm 3 provides an overview.

Traning stage. The training stage mimics Algorithm 2 but uses moving blocks to re-sample the initial sample, see Line 5 in Algorithm 2. Let $y_i^* = (y_{1,i}^*, y_{2,i}^*, \dots, y_{T,i}^*)$ be the initial sample from the true DGP. We perform a blocking procedure identical to the moving block bootstrap. Define each of the $(T - b_1 - 1)$ overlapping blocks by $B_j^* = (y_{1j} = y_{1+j,i}^*, \dots, y_{2j} =$

Algorithm 3 Generative Bootstrap

```
1: for  $r = 1, 2, \dots, R$  do: ▷ Training stage
2:   Use Algorithm 2 but batches consist of resampled blocks with size  $b_1$ .
3: end for
4:
5: for  $s = 1, 2, \dots, S$  do: ▷ Sampling stage
6:    $x \leftarrow \text{Sample}(\text{model}, b_2)$ 
7:    $\text{estimates}[s] \leftarrow \text{Statistic}(x)$ 
8: end for
```

$y_{1+j+b_1,i}^*$) where the block size is $b_1 < T$. A batch of training data is given by randomly sampling n_b blocks from $\{B_1^*, B_2^*, \dots, B_{T-b_1-1}^*\}$ without replacement, denote this batch of true blocks by \mathcal{Y}^* .

Next, we sample the generator noise (see Line 3 of Algorithm 2) from a multivariate standard normal distribution with an identity variance-covariance matrix, but the distribution F_Z could be selected arbitrarily. To generate a sample path of length b_1 we need $(b_1 + p)$ noise terms where p is the receptive field in the DTC layers – see Equation 10. The noise terms are used to generate a block sample $B_j = (G(z_1, \dots, z_p; \theta_G), G(z_{1+1}, \dots, z_{p+1}; \theta_G), \dots, G(z_{b_1}, \dots, z_{b_1+p}; \theta_G))$, see Line 4 of Algorithm 2, and n_b of such blocks are generated to form a batch of fake blocks, denote them by \mathcal{Y} . The true and fake samples are fed to the discriminator and it tries to distinguish between them. This requires that the blocks in \mathcal{Y}^* and \mathcal{Y} have the same size. This procedure of sampling true and fake blocks and feeding them to the discriminator constitutes the training stage. In practice, we iterate over Equation D1-G1 until the losses stabilise. Equation D1 requires both a fake and true batch per iteration, while Equation G1 needs only a fake batch.

Sampling stage. Let $G(\cdot; \hat{\theta}_G)$ be the learned generator from the training stage. Once trained, the generator should produce samples mimicking the true DGP that generated the initial sample y_i^* . To generate a sample of length b_2 , we first sample a sequence of noise vectors from F_Z

$$z_i = (z_{1,i}, z_{2,i}, \dots, z_{b_2+p,i}), \quad z_{t,i} \sim F_Z$$

where p is again given in Equation 10. As in the training stage, F_Z is a multivariate standard normal distribution with an identity variance-covariance matrix. Any distribution could be used, the important point is that the training and sampling stages use the *same* distribution for F_Z . Next we obtain a generated sample path y_i by passing the noise vectors through the learned generator,

$$y_i = (G(z_{1,i}, \dots, z_{p,i}; \hat{\theta}_G), G(z_{1+1,i}, \dots, z_{p+1,i}; \hat{\theta}_G), \dots, G(z_{b,i}, \dots, z_{b_2+p,i}; \hat{\theta}_G)).$$

A single sequence of innovation vectors $z_i = (z_{1,i}, \dots, z_{b_2+p,i})$ generates one sample path y_i of length b_2 . We can repeat this process to obtain an arbitrary number of sample paths.

Under the proposed TC-architecture the generator can sample a block of any length from the underlying process and hence we are not restricted to the block size on which the model was trained, i.e. it is perfectly acceptable if $b_1 \neq b_2$. This does not necessarily hold for all choices of architecture, e.g. a fully-connected network would not have this property. This is a very attractive feature of the TC and GAN approach as it alleviates the need to stack individual blocks in a way that might break the dependence structure of the time series. We can simply choose the sampling block size to be equal to the size of the initial sample path, so $b_2 = T$.

When $b_2 < T$ we refer to it as *blocked sampling*, while $b_2 = T$ is called *complete sampling*.

Bootstrap statistics. Let $G(\cdot; \hat{\theta}_G)$ be the learned generator from the training stage that has been trained on a single initial sample y_i^* from the true DGP. We now discuss how to calculate bootstrap statistics on the GAN samples. Assume that we are interested in parameter ϕ which has a suitable estimator $\hat{\phi}$. We use the sampling procedure from the previous section to obtain m samples from the learned generator $G(\cdot; \hat{\theta}_G)$, denote these samples by (y_1, y_2, \dots, y_m) where $y_i = (y_{1,i}, \dots, y_{T,i}), i = 1, \dots, m$. Each y_i is considered a realisation of the DGP that produced the initial training sample for the GAN. We calculate the bootstrap statistics $\hat{\phi}_i \equiv \hat{\phi}(y_i), i = 1, \dots, m$ resulting in m estimates $(\hat{\phi}_1, \hat{\phi}_2, \dots, \hat{\phi}_m)$.

Similar to conventional bootstrapping (Efron, 1981), the GB variance estimate of $\hat{\phi}$ is

$$\hat{\sigma}_{GB,\hat{\phi}} = \frac{1}{m} \sum_i (\hat{\phi}_i - \hat{\phi}_{GB})^2. \quad (11)$$

The $(1 - \alpha)$ GB confidence interval (CI) for ϕ is the $(1 - \alpha)$ percentile CI (Efron, 1981) constructed using the empirical quantiles² $(\alpha/2, 1 - \alpha/2)$ of $(\hat{\phi}_i)_i$,

$$\hat{I}_{\phi,1-\alpha} = \left[\hat{\phi}_{(\alpha/2)}, \hat{\phi}_{(1-\alpha/2)} \right]. \quad (12)$$

4. SIMULATIONS

In this section we will illustrate the performance of the GB by using simulations and by making comparisons to the established CBB approach for bootstrapping dependent processes. For simplicity of exposition we base our illustrations on the AR(1) as the data generating process.

4.1. AR(1) process

The simulation design is as follows. The true DGP is a zero mean and stable AR(1) process

$$y_t = \phi y_{t-1} + \epsilon_t, \quad \epsilon_t \sim N(0, 1) \quad (13)$$

with $\phi = 0.5, 0.8, 0.9$. For each replication, a sample path of length $T = 1,000$ is generated from Equation 13. This sample is used to train the GAN with a training block size of $b_1 = 150$ and batch size $n_b = 64$. Once training is complete, we sample 10,000 sample paths from the GAN. These samples are used for two purposes:

(a) we compare the samples generated by the proposed GAN to the known properties of the DGP under complete sampling $b_2 = 1,000$. We use the generated samples to estimate the

²A possible improvement on this confidence interval would be the bias-correction techniques outlined in (Efron, 1987).

autocorrelation (ACF) and partial autocorrelation (PACF) functions over 1,000 replications.

(b) we compare GB and the CBB for confidence interval estimation, i.e., empirical coverage, of the least-squares estimator $\hat{\phi}_{LS}$ of ϕ . The GB is run for 1,000 replications and the CBB is run for 5,000 replications. The CBB resamples from the same initial sample as is used to train the GB. We consider CBB block sizes $b_1 = 50, 100, 150$. The GB training block size equals 150. The number of replications for GB is lower as the simulation time is considerably higher than for CBB. A GB replication takes around 20-30 minutes while it is less than a minute for CBB. It is important to note that, in both the CBB and GB, we do not specify the dynamics of the true DGP. The GB assumes that the dynamics can be approximated by some functions of the noise vectors but these functions are not fully specified.

The following section details the hyper parameters and training of the GAN. The two succeeding sections discuss the simulation results – first the correlation structure of the generated samples and secondly the higher-level statistics in a bootstrapping context.

GAN implementation details. We discuss the hyper parameters and network design of the GAN.

The discriminator has 6 temporal convolution layers with common kernel size 2 and dilations (1, 2, 4, 8, 16). The filters are (8, 16, 32, 32, 64, 64). The output from temporal layers number 1, 2, and 6 are run through adaptive max pooling (AMP) with feature size 16 and concatenated into a feature vector of size 48. This is followed by two fully connected layers that regress into a single output unit. All layers use leaky ReLU activation (Maas et al., 2013) except for the final layer which has no activation function. The leaky ReLU avoids the zero-gradient problem of conventional ReLUs during training (Maas et al., 2013). The generator has 6 temporal convolution layers that directly outputs a sample path. The filters are (128, 64, 32, 32, 16, 1). Except for the last layer, all layers use the Tan activation function as it – unlike ReLU – is symmetric. The total number of (trainable) discriminator parameters is 233,609 while the generator has 89,921 (trainable) parameters.

The generator noise is sampled from a multivariate standard normal distribution with an identity variance-covariance matrix. To generate a sample path of length b we need $(b + p)$ noise terms where p is the receptive field size in the DTC layers – see Equation 10 – and b is either b_1 or b_2 corresponding to training or sampling stage. The dimension of the noise term is a hyper parameter and can be chosen arbitrarily, in our simulations we use 256. If we stack all the noise terms needed to produce a sample path of size b then we obtain a $(b + p) \times 256$ matrix with iid standard normal distributed entries.

The GAN is trained for 5,000 steps based on a single sample from the DGP. We do not employ any (early) stopping criterion, so the GAN is always trained till the final step. The training involves iteratively minimising the batch losses, see Equation D1-G1. Instead of stochastic gradient descent, we use the more complex Adam algorithm as it can accelerate training, see (Kingma and Ba, 2014). Table 1 in the Appendix lists all hyper parameters for the GAN in this paper.

(a) ACF and PACF properties of the GAN samples. We compare the samples produced by the GAN and CBB against the theoretical properties of the AR(1) process.³ A common discussion is whether the GAN has learned to produce new samples or if it simply reproduces the original samples perfectly. If the generative model learned to perfectly replicate the original sample then the method would perform approximately on-par with CBB. Favourable bootstrapping characteristics of the GAN relative to CBB could indicate that the GAN has an advantage in capturing the dynamics of the DGP and that it does not simply replicate blocks of the original sample.

The theoretical autocorrelation function (ACF) for an AR(1) process is given by $\gamma(j) \equiv \text{Cor}(y_t, y_{t-j}) = \phi^j$ for $\phi = 0.5, 0.8, 0.9$. We estimate the ACF using generated samples under the complete sampling scheme. The ACF estimates are averaged over 1,000 replications. Figure 2 plots the estimated ACF (full line) against the theoretical ACF (dashed line). In Figure 2 we have also included the interquartile range (IQR) for the theoretical ACF and

³For the implementation of the CBB we have used the Python library by Sheppard (2020).

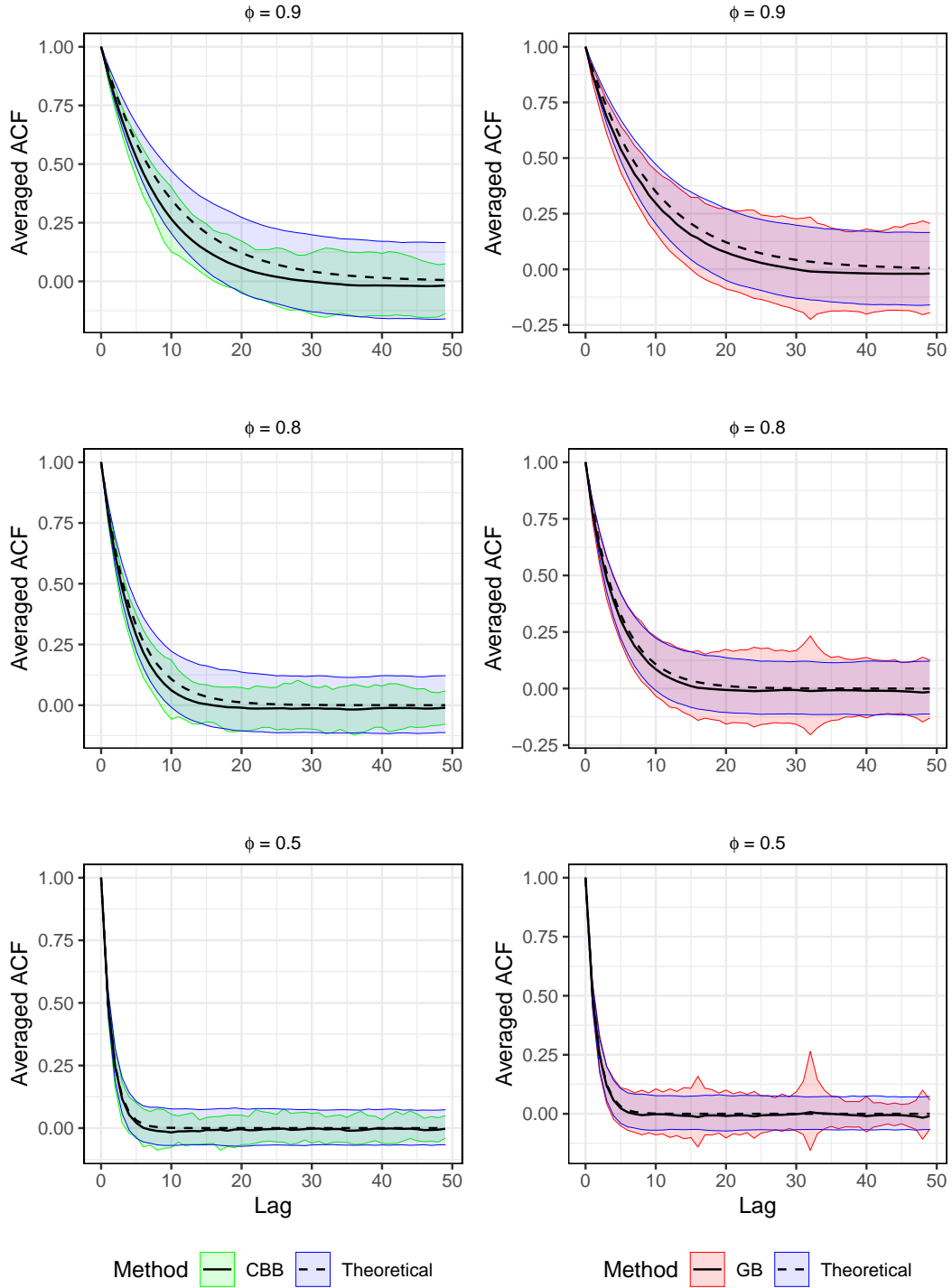


Figure 2: Theoretical (dashed line, blue ribbon) and sample autocorrelation functions for CBB (green ribbon) and GAN (red ribbon) resamples when $\phi = 0.5, 0.8, 0.9$. Block size for CBB is 150 and training block size for GAN is 150. The ACF estimates and confidence bands are based on 1,000 replications of the generative model with 10,000 samples per replication.

for the ACF estimated across the 1,000 replications. If the GAN has learned the dynamics of the AR(1) process, then the estimated and the theoretical ACF should be similar and the theoretical and the estimated IQR should be overlapping. Clearly, for higher values of the autoregressive parameter ϕ the persistency of the process is stronger and challenges the GAN to learn longer range dependencies.

From Figure 2 the estimated ACFs are close to their theoretical counterparts for all lags when $\phi = 0.5$. For $\phi = 0.8$ there is a small upwards bias in the estimated ACFs that is larger for the CBB, particularly, for the intermediate range of lag lengths, i.e, lags 5-20. For $\phi = 0.9$ there is a small but noticeable bias in the estimated ACFs for all lags considered for both CB and CBB. The bias is again uniformly larger for the CBB. Importantly, all theoretical ACFs are well within the IQR of the estimated ACFs.

For $\phi = 0.5$ the estimated IQR of the CBB (green ribbon) is almost identical to the theoretical IQR (blue ribbon). However, for $\phi = 0.8$ and $\phi = 0.9$ the upper limit of the estimated IQRs for CBB seem to be considerably downward biased for all lags. Noticably, the estimated IQRs for CB (red ribbon) appear to be much less sensitive to the value of ϕ and the estimated IQRs for CB are only marginally wider than the theoretical IQRs. We find these results very encouraging.

Next we turn to the partial autocorrelation function (PACF). For an AR(p) process the PACF is zero for lags larger than p . The AR(1) process is expected to have PACF equal to ϕ at lag 1 and zero PACF for all following lags. Figure 3 depicts the estimated PACF using the GAN samples and plots it against the theoretical PACF (horizontal dotted line). The black horizontal marks denote the estimated IQRs. The estimated PACFs have the expected behaviour for $\phi = 0.5, 0.8$ with values close to 0.5 and 0.8 at lag 1 respectively and with values very close to zero for all remaining higher order lags. For the highly persistent case $\phi = 0.9$ the estimated PACF is slightly more imprecise with a notable non-zero PACF at lag 2. However, overall, the PACF based on the GAN sample clearly suggests that the underlying time series under consideration is a highly persistent AR(1) process.

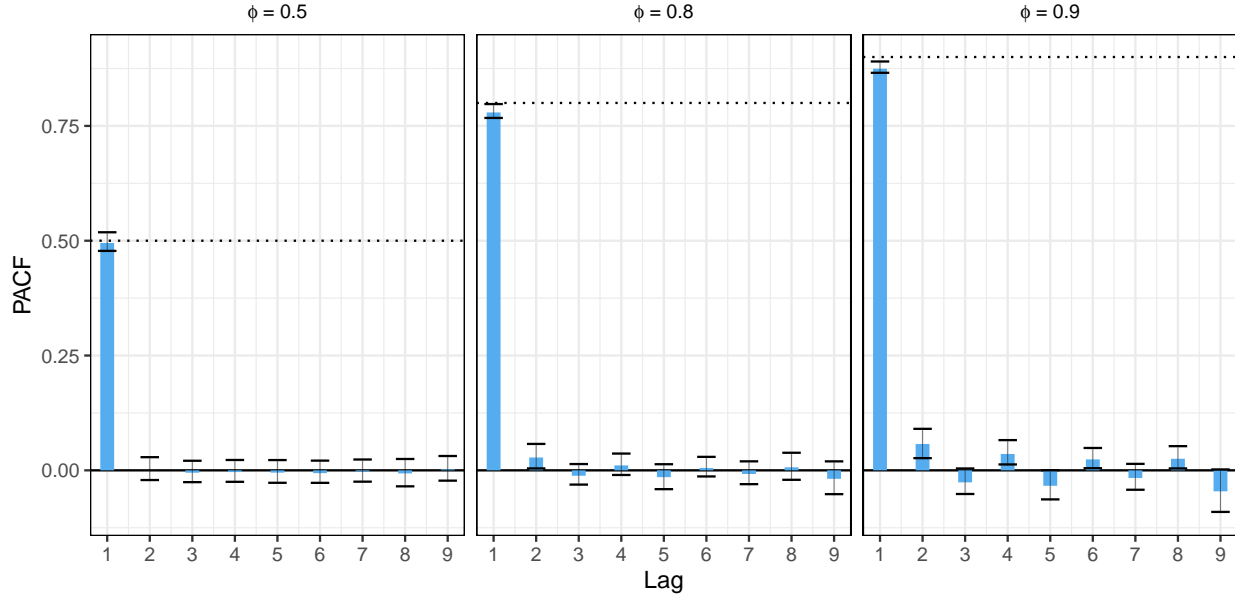


Figure 3: Top panel: Sample partial autocorrelation function (blue bars) for $\phi = 0.5$, $\phi = 0.8$ and $\phi = 0.9$. The estimates are based on 1,000 replications of the generative model with 10,000 samples per replication. The black marks depict the interquartile range (IQR) of the estimates across the 1,000 replications.

(b) Bootstrapping the least-squares estimator. We apply the GAN for re-sampling and examine if it recovers higher-level statistics, in particular, the sampling distribution of the usual least-squares (LS) estimator $\hat{\phi}_{LS}$ of the autoregressive parameter ϕ .

The simulation design is identical to that initially described. We obtain 10,000 sample paths from the GAN across 1,000 replications with $\phi = 0.5, 0.8, 0.9$. For each replication, the GB variance of $\hat{\phi}_{LS}$ and the GB confidence intervals are constructed as in Section 3. Using the usual asymptotic approximation, the LS estimator $\hat{\phi}_{LS}$ has asymptotic variance $(1 - \phi^2)^{-1}$.

Figure 4 contains the main simulation results for the GB using complete sampling ($b_2 = 1,000$). For values of ϕ in the range $0 - 0.75$ the GB in general produces far better empirical coverage than CBB for all nominal confidence levels, but in particular for the levels 0.99, 0.95, and 0.9. For the highly persistent processes none of the re-sampling methods considered have good empirical coverage. In these cases the empirical coverage of the GB is at par with the CBB with a block size equal to 100. Not surprisingly, the CBB with the largest block

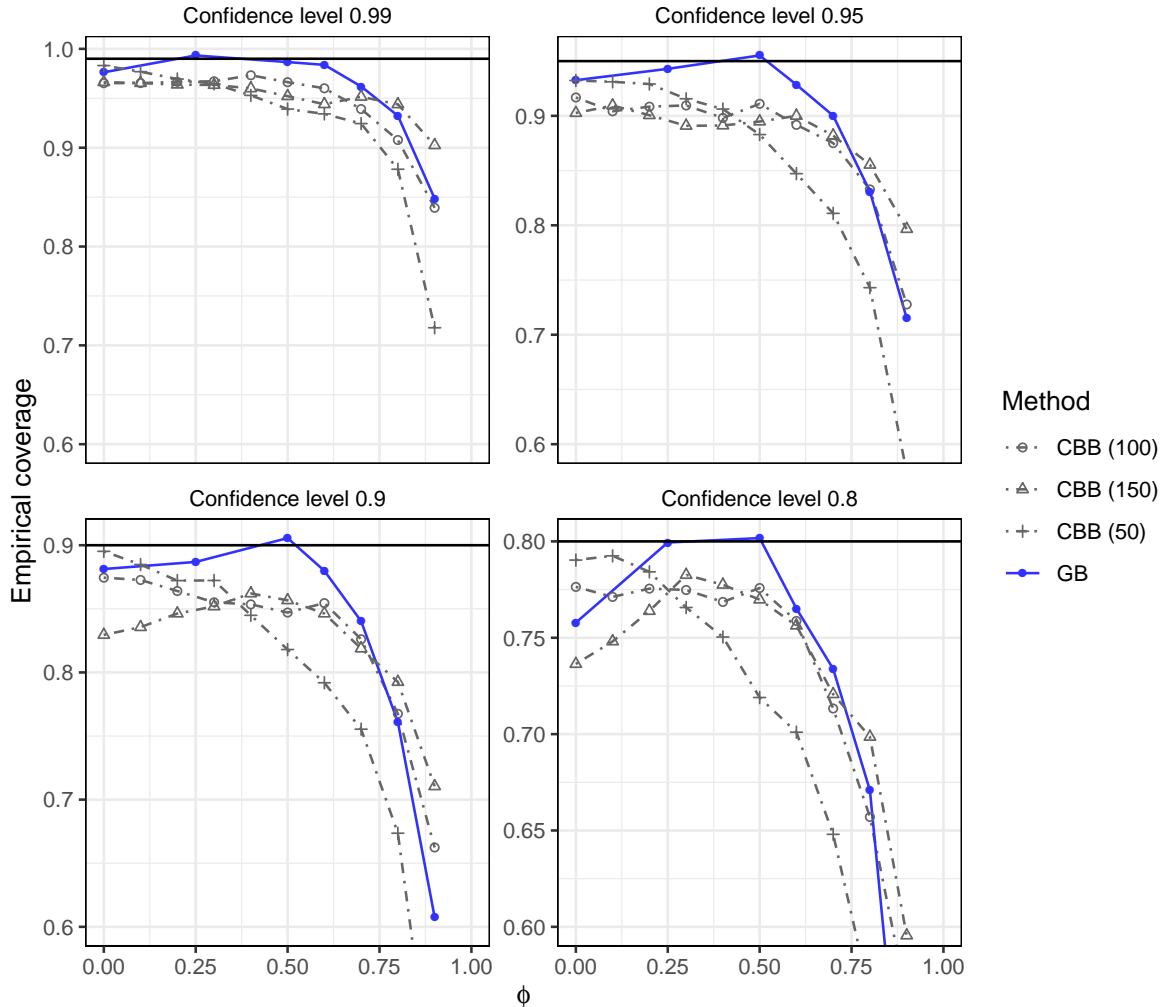


Figure 4: Empirical coverage of percentile confidence intervals – with nominal confidence levels (0.99, 0.95, 0.90, 0.80) – for the CBB and the GB (using complete sampling) under different choices of the autoregressive parameter ϕ . The horizontal lines depict the corresponding desired nominal confidence levels.

size (=150) here has the best coverage.

It is very likely that the performance of the GB for highly persistent processes could be improved by increasing the number of layers in temporal convolution network. Recall, that a temporal convolution network with d layers and fixed kernel size 2 accounts for at-most $2^{d+1} - 1$ lags (the receptive field), hence an increase in d might rectify this problem. How to select the optimal number of d layers in the GB procedure as a function of the persistence

of original process is ongoing work.

5. CONCLUDING REMARKS

GANs provide a promising approach for simulating time series data. Our results suggest that GANs can accurately learn the dynamics of common autoregressive time series processes using temporal convolutional networks. In addition, it seems compelling that the GAN appears to improve empirical coverage in bootstrapping of dependent data when compared to the circular block bootstrap. This gives credibility to the use of GANs on data from time series processes that are unknown.

It is important to note that the various dependent bootstraps have a theoretical justification and their properties have been theoretically derived, see e.g. the overview in (Lahiri, 1999). The GAN and GB currently do not have this theoretical reassurance.

The GAN relies on a large number of hyper parameters and design choices. We have not investigated how sensitive our results are to these but research on this is ongoing. We have used sensible defaults for batch sizes, learning rates, gradient penalty, update iteration scheme, activation functions, optimiser but these are by no means optimal choices. This is a general shortcoming in the GAN literature and little is known about how to optimally choose these values.

Our simulations also rely on a simple and basic time series process. It would be fruitful to consider the performance on more general stationary processes (ARMA) and in settings where the error term has stochastic variance, e.g. GARCH.

REFERENCES

- Arjovsky, Martin, Soumith Chintala, and Léon Bottou (2017). “Wasserstein GAN”. In: *arXiv preprint 1701.07875*. URL: <https://arxiv.org/abs/1701.07875>.
- Athey, Susan et al. (2019). “Using Wasserstein Generative Adversarial Networks for the Design of Monte Carlo Simulations”. In: *arXiv preprint 1909.02210*. URL: <https://arxiv.org/abs/1909.02210>.
- Biau, G., B. Cadre, et al. (2018). “Some Theoretical Properties of GANs”. In: *arXiv preprint 1803.07819 (forthcoming in Annals of Statistics)*. URL: <https://arxiv.org/abs/1803.07819>.
- Biau, Gérard, Maxime Sangnier, and Ugo Tanielian (2020). “Some Theoretical Insights into Wasserstein GANs”. In: URL: <https://arxiv.org/abs/2006.02682>.
- Borovykh, Anastasia, Sander Bohte, and Cornelis W. Oosterlee (2017). “Conditional Time Series Forecasting with Convolutional Neural Networks”. In: *arXiv preprint 1703.04691*. URL: <https://arxiv.org/abs/1703.04691>.
- Efron, Bradley (1981). “Nonparametric Standard Errors and Confidence Intervals”. In: *The Canadian Journal of Statistics / La Revue Canadienne de Statistique* 9.2, pp. 139–158.
- (1987). “Better Bootstrap Confidence Intervals”. In: *Journal of the American Statistical Association* 82.397, pp. 171–185.
- Goodfellow, Ian, Yoshua Bengio, and Aaron Courville (2016). *Deep learning*. MIT press.
- Goodfellow, Ian, Jean Pouget-Abadie, et al. (2014). “Generative Adversarial Nets”. In: *Advances in neural information processing systems*, pp. 2672–2680.
- Gulrajani, Ishaan et al. (2017). “Improved training of Wasserstein GANs”. In: *Advances in neural information processing systems*, pp. 5767–5777.
- Haas, Moritz and Stefan Richter (2020). “Statistical analysis of Wasserstein GANs with applications to time series forecasting”. In: URL: <https://arxiv.org/abs/2011.03074>.
- Heusel, Martin et al. (2017). “GANs Trained by a Two Time-Scale Update Rule Converge to a Nash Equilibrium”. In: *CoRR* abs/1706.08500. URL: <http://arxiv.org/abs/1706.08500>.
- Hornik, Kurt, Maxwell Stinchcombe, and Halbert White (1990). “Universal approximation of an unknown mapping and its derivatives using multilayer feedforward networks”. In: *Neural networks* 3.5, pp. 551–560.
- Hyland, Stephanie L, Cristóbal Esteban, and Gunnar Rätsch (2017). “Real-valued (medical) time series generation with recurrent conditional GANs”. In: *arXiv preprint 1706.02633*. URL: <https://arxiv.org/abs/1706.02633>.
- Kaji, Tetsuya, Elena Manresa, and Guillaume Pouliot (2018). *Deep Inference: Artificial Intelligence for Structural Estimation*. Tech. rep. URL: <https://events.barcelonagse.eu/live/files/2773-elenamanresa66433pdf>.
- Kingma, Diederik P and Jimmy Ba (2014). “Adam: A method for stochastic optimization”. In: *arXiv preprint 1412.6980*. URL: <https://arxiv.org/abs/1412.6980>.
- Kunsch, Hans R (1989). “The jackknife and the bootstrap for general stationary observations”. In: *The annals of Statistics*, pp. 1217–1241.
- Lahiri, Soumendra N (1999). “Theoretical comparisons of block bootstrap methods”. In: *Annals of Statistics*, pp. 386–404.

- Liu, Regina Y, Kesar Singh, et al. (1992). “Moving blocks jackknife and bootstrap capture weak dependence”. In: *Exploring the limits of bootstrap* 225, p. 248.
- Maas, Andrew L, Awni Y Hannun, and Andrew Y Ng (2013). “Rectifier nonlinearities improve neural network acoustic models”. In: *Proc. icml*. Vol. 30. 1.
- Oord, Aaron van den et al. (2016). “WaveNet: A Generative Model for Raw Audio”. In: *arXiv preprint 1609.03499*. URL: <https://arxiv.org/abs/1609.03499>.
- Paparoditis, Efstathios and Dimitris N. Politis (2001). “Tapered Block Bootstrap”. In: *Biometrika* 88.4, pp. 1105–1119.
- Politis, Dimitris N and Joseph P Romano (1992). “A circular block-resampling procedure for stationary data”. In: *Exploring the limits of bootstrap* 2635270.
- Radford, Alec, Luke Metz, and Soumith Chintala (2015). “Unsupervised representation learning with deep convolutional generative adversarial networks”. In: *arXiv preprint 1511.06434*. URL: <https://arxiv.org/abs/1511.06434>.
- Salimans, Tim et al. (2016). “Improved Techniques for Training GANs”. In: *CoRR* abs/1606.03498. URL: <http://arxiv.org/abs/1606.03498>.
- Sen, Rajat, Hsiang-Fu Yu, and Inderjit Dhillon (2019). “Think Globally, Act Locally: A Deep Neural Network Approach to High-Dimensional Time Series Forecasting”. In: *arXiv preprint 1905.03806*. URL: <https://arxiv.org/abs/1905.03806>.
- Shao, Xiaofeng (Mar. 2010). “The Dependent Wild Bootstrap”. In: *Journal of the American Statistical Association* 105.489, pp. 218–235.
- Sheppard, Kevin (2020). “bashtage/arch: Release 4.15 (Version 4.15).” In: *Zenodo*. URL: <https://doi.org/10.5281/zenodo.593254>.
- Smith, Kaleb E and Anthony O Smith (2020). “Conditional GAN for timeseries generation”. In.
- Wiese, Magnus et al. (Apr. 2020). “Quant GANs: deep generation of financial time series”. In: *Quantitative Finance*, pp. 1–22.
- Yu, Fisher and Vladlen Koltun (2015). “Multi-Scale Context Aggregation by Dilated Convolutions”. In: *arXiv preprint 1511.07122*. URL: <https://arxiv.org/abs/1511.07122>.

APPENDIX

Hyper parameter	Value
Discriminator learning rate, lr_d	0.00025
Generator learning rate, lr_d	0.00025
Gradient penalty, λ	20
Batch size, n_b	64
Discriminator init updates, N_{init}	50
Discriminator updates, $N_{discriminator}$	5
Generator updates, $N_{generator}$	1
Initial weight distribution	N(0, 0.02)
Adam optimiser, ϵ	10^{-8}
Adam optimiser, β_1	0.5
Adam optimiser, β_2	0.9

Table 1: Generative Bootstrap (GB) hyper paramaters.